Recent oscillation analysis results from Daya Bay

Jie Zhao[*][†]

(On behalf of the Daya Bay Collaboration)
E-mail: zhaojie@ihep.ac.cn

The Daya Bay Reactor Antineutrino Experiment was designed to precisely determine the neutrino mixing angle θ_{13} utilizing eight functionally identical electron-antineutrino ($\overline{\nu}_e$) detectors. Using 217 days of data with six detectors, and 404 days with eight detectors, 150255 (613813 and 477144) antineutrino candidates were detected in the far hall (near halls). Combining the information from the neutrino rate deficit and the spectral distortion, the Daya Bay experiment made an improved measurement of the oscillation parameters that drive electron antineutrino disappearance at short distance: $\sin^2 2\theta_{13} = 0.084 \pm 0.005$ and $|\Delta m_{ee}^2| = 2.44_{-0.11}^{+0.10} \times 10^{-3}$ eV^2.

In this paper, we will describe the recent oscillation analysis results, focusing on the improvement of the detector energy response and backgrounds, the consistency of the performance across all detectors, and the combined fitting to the six and eight detector data set.

---

[*]Speaker.

[†]Institute of High Energy Physics, Beijing, China.

1. Introduction

Neutrinos are elementary particles in the Standard Model of particle physics. There are three flavors of neutrinos, known as υ_e, υ_μ and υ_τ. Each neutrino flavor state is a superposition of three mass eigenstates (υ_1, υ_2 and υ_3), which undergo quantum interference during travel. This causes the probability of detecting a certain type of flavor state to change as a function of the distance traveled and the energy, a phenomenon known as neutrino oscillation. The amplitude of the oscillation is determined by three mixing angles θ_{12}, θ_{23} and θ_{13}, and the oscillation frequency is determined by the difference of the squared neutrino masses, $\Delta m_{ij}^2 = m_i^2 - m_j^2$.

In the last decades, θ_{12}, θ_{23}, Δm_{21}^2 and Δm_{32}^2 were determined through the combined measurements done by solar, atmospheric, reactor and accelerator experiments [1]. Prior to 2011, the best knowledge of the remaining angle θ_{13} was just an upper limit of $\sin^2 2\theta_{13} <$0.15 at 90% confidence level [2]. In Mar. 2012, with 55 days data collected from six antineutrino detectors (ADs), the Daya Bay Experiment reported the first definite observation of a non-zero value of θ_{13} with 5.2 standard deviations [3]. In Oct. 2013, with 217 days of six-AD data, Daya Bay improved the measurement of θ_{13} and reported the first measurement of the effective squared mass difference $|\Delta m_{ee}^2|$ (a combination of Δm_{32}^2 and Δm_{31}^2) in the electron antineutrino disappearance channel [4].

In the summer 2012, the remaining two ADs were installed and data-taking with all eight detectors begun on Oct 19, 2012. By the end of 2013, more than three times the statistics of the six-AD data period were accumulated. Both relative differences of the detector performance and the background uncertainty were reduced with an improved reconstruction and the increased statistics. In addition, two out of three AmC neutron sources were removed from each far site detector during the summer maintenance in 2012, significantly reducing the AmC induced correlated background.

This paper begins with a brief introduction to the Daya Bay Experiment. A description of the analysis with 621 days of data follows, including the details on the $\overline{\upsilon}_e$ event selection, the relative detector efficiency, and the backgrounds. The best estimates of the oscillation parameters resulting from a rate and spectral shape analysis are presented at the end, before a short summary.

2. The Daya Bay Experiment

The Daya Bay experiment was designed to provide the most precise measurement of θ_{13} among existing and near future experiments, with a sensitivity to $\sin^2 2\theta_{13} < 0.01$ at the 90% confidence level [5].

To achieve this goal, a near-far arrangement of ADs allowing to compare the measured $\overline{\upsilon}_e$ rates at various baselines was implemented. Performing a relative measurement allows to almost fully cancel reactor and relative detector systematic uncertainties. In the near (far) site, two (four) identical antineutrino detectors are installed in pure-water pools. The water pool and the resistive plate chambers (RPC) on the top form the muon veto system, shielding the detectors from radioactivity in the surrounding rocks and allowing to tag cosmic-ray muons. Each AD is comprised of three volumes separated by acrylic vessels. The innermost vessel holds 20 tons of gadolinium doped liquid scintillator (Gd-LS) as the antineutrino target. The scintillator volume is filled with 22 tons of LS for detecting gamma-rays that escape from the target volume. The outer volume contains 37 tons of mineral oil that provide optical homogeneity and that shield the inner volumes from

radiation, such as the one originating in the glass of the 192 photomultiplier tubes (PMTs). Three automated calibration units (ACUs) containing radioactive sources and LEDs are installed on top of each detector, at different distances from the central axis.

$\overline{v}_e$ are detected via the inverse-beta decay (IBD) reaction: $\overline{v}_e + p \rightarrow e^+ + n$. The positron deposits energy and annihilates with an electron almost immediately, while the neutron is captured by Gd or H with a mean capture time of about 28 μs in the 0.1% Gd-doped LS. A neutron captured by Gd emits gammas with a total energy of about 8 MeV, and a neutron captured by H emits 2.2 MeV gamma. The time and energy correlations allow to identify $\overline{v}_e$ with very little background.

3. Event Selection

3.1 IBD Selection

IBD events are selected with the following criteria: $0.7 < E_p < 12.0$ MeV, $6.0 < E_d < 12.0$ MeV, and $1 < \Delta t < 200$ μs, where $E_p(E_d)$ is the prompt (delayed) energy and $\Delta t = t_d - t_p$ is the time difference between the prompt and delayed signals. The prompt-delayed pair is vetoed if the delayed signal is within 600 μs after a water pool trigger. If a muon deposits > 20 MeV energy in an AD, the veto window is extended to 1 ms due to the increased probability of multiple neutrons. If a muon deposits > 2.5 GeV energy in an AD, the veto window is extended to 1 s to reject long-lived cosmogenic backgrounds. A multiplicity cut that requires no additional > 0.7 MeV trigger in the time range $(t_p - 200\mu s, t_d + 200\mu s)$ is also applied.

Five kinds of background are identified that can mimic the prompt and delayed signals of $\overline{v}_e$: accidental coincidences of two uncorrelated signals, β-n cascade decays of $^9Li/^8He$ produced by muons passing through the ADs, fast-neutrons produced by muons outside the ADs, $^{13}C(\alpha,n)^{16}O$ interactions, and neutrons inelastically scattering with nuclei in the shielding material from the retracted Am-C neutron source in the ACUs. The accidental coincidence, correlated background from $^9Li/^8He$ and $^{13}C(\alpha,n)^{16}O$ backgrounds are determined using the same methods as before [3].

The fast neutron background is estimated using a model independent measurement. The RPC-only and OWS tagged fast neutron spectrum are used in the estimation. After scaling to data, the mean value of the two spectra are regarded as our fast neutron background. The uncertainty is determined by the difference between the new measurement and the previous estimate, and it was reduced by a factor of 2 compared to the previous method.

The AmC correlated background is estimated through a Monte Carlo simulation benchmarked with single gamma and a special calibration dataset acquired using a strong AmC source with a neutron rate about 78 times higher than the regular one. During the summer 2012, two out of three AmC sources were removed in each far site AD. Thus the AmC background rate was reduced to about two thirds from each far site AD.

Table 1 and Table 2 summarize the main numbers of the six-AD and eight-AD datasets. The background and IBD rates are corrected for efficiency. The ratio of background and signal is about 2% (3%) for the near (far) site.

3.2 Efficiencies and uncertainties

Table 3 is a summary of absolute efficiencies and their correlated and uncorrelated systematic

Table 1: IBD selection results for the six-AD period.

	AD1	AD2	AD3	AD4	AD5	AD6
IBD candidates	101998	103137	93742	13889	13814	13645
DAQ live time(day)	190.989		189.623	189.766		
ε_μ	0.8234	0.8207	0.8576	0.9811	0.9811	0.9808
ε_m	0.9741	0.9745	0.9757	0.9744	0.9742	0.974
Accidentals(/day)	9.53 ± 0.10	9.29 ± 0.10	7.40 ± 0.08	2.93 ± 0.03	2.87 ± 0.03	2.81 ± 0.03
Fast neutron(/day)	0.78 ± 0.12		0.54 ± 0.19	0.05 ± 0.01		
9Li/8He(/day)	2.8 ± 1.5		1.7 ± 0.9	0.27 ± 0.14		
AmC correlated(/day)	0.27 ± 0.12	0.25 ± 0.11	0.27 ± 0.12	0.22 ± 0.10	0.21 ± 0.10	0.21 ± 0.09
$^{13}C(\alpha,n)^{16}O$(/day)	0.08 ± 0.04	0.07 ± 0.04	0.05 ± 0.03	0.05 ± 0.03	0.05 ± 0.03	0.05 ± 0.03
IBD rate(/day)	652.38 ± 2.58	662.02 ± 2.59	580.84 ± 2.14	73.04 ± 0.67	72.71 ± 0.67	71.88 ± 0.67
side-by-side ibd rate ratio	0.985 ± 0.005					

Table 2: IBD selection results for the eight-AD period.

	AD1	AD2	AD3	AD8	AD4	AD5	AD6	AD7
IBD candidates	202461	206217	193356	190046	27067	27389	27032	27419
DAQ live time(day)	374.447		378.407		372.685			
ε_μ	0.8255	0.8223	0.8574	0.8577	0.9811	0.9811	0.9808	0.9811
ε_m	0.9746	0.9749	0.9759	0.9756	0.9762	0.976	0.9757	0.9758
Accidentals(/day)	8.62 ± 0.09	8.76 ± 0.09	6.43 ± 0.07	6.86 ± 0.07	1.07 ± 0.01	0.94 ± 0.01	0.94 ± 0.01	1.26 ± 0.01
Fast neutron(/day)	0.78 ± 0.12		0.54 ± 0.19		0.05 ± 0.01			
9Li/8He(/day)	2.8 ± 1.5		1.7 ± 0.9		0.27 ± 0.14			
AmC correlated(/day)	0.20 ± 0.09	0.21 ± 0.10	0.18 ± 0.08	0.22 ± 0.10	0.06 ± 0.03	0.04 ± 0.02	0.04 ± 0.02	0.07 ± 0.03
$^{13}C(\alpha,n)^{16}O$(/day)	0.08 ± 0.04	0.07 ± 0.04	0.05 ± 0.03	0.07 ± 0.04	0.05 ± 0.03	0.05 ± 0.03	0.05 ± 0.03	0.05 ± 0.03
IBD rate(/day)	659.58 ± 2.12	674.36 ± 2.14	601.77 ± 1.67	590.81 ± 1.66	74.33 ± 0.48	75.40 ± 0.49	74.44 ± 0.48	75.15 ± 0.49
side-by-side ibd rate ratio	0.978 ± 0.004		1.019 ± 0.004					

uncertainties. In our relative measurement, only the uncorrelated uncertainties (dominated by the delayed energy cut and the Gd capture ratio) contribute to the final error.

Table 3: Summary of absolute efficiencies, and correlated and uncorrelated systematic uncertainties.

	Efficiency	Uncertainty	
		Correlated	Uncorrelated
Target Protons		0.47%	0.03%
Flasher cut	99.98%	0.01%	0.01%
Delayed Energy cut	92.7%	0.97%	0.12%
Prompt Energy cut	99.81%	0.10%	0.01%
Capture time cut	98.70%	0.12%	0.01%
Gd capture ratio	84.2%	0.95%	0.10%
Spill-in correction	104.9%	1.50%	0.02%
Combined	80.6%	2.1%	0.2%

The uncorrelated uncertainty of delayed energy cut comes from relative energy scale uncertainty at 6 MeV. Fig 1 shows the asymmetries in energy response as a function of energy in eight ADs. The data points are from calibration sources and uniformly distributed sources. The energy scale was determined by the position of the ^{60}Co and AmC sources. Recently, an AD by AD correction for the energy nonlinearity between ^{60}Co and neutron capture on Gd was implemented.
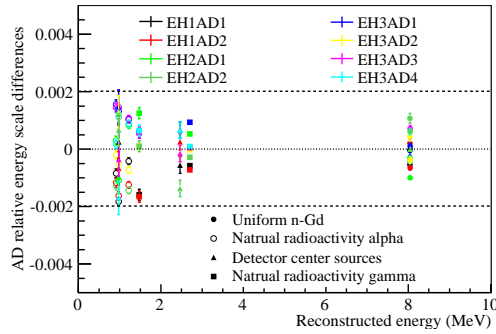
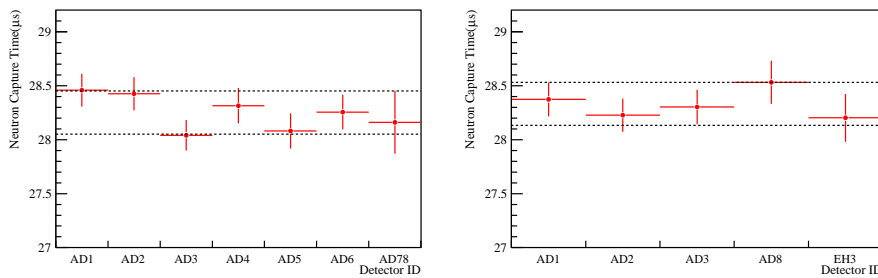**Figure 1:** Asymmetries in energy response for all eight ADs.

Figure 2: Neutron capture time for AmC (top) and IBD (bottom) samples in eight ADs.

With this improved reconstruction method, the variation in reconstructed energy is improved from 0.35% to 0.2% between the ADs.

The neutron capture times for eight ADs are shown in Fig 2. The results of all ADs data fall inside 0.2 μs uncertainty band within the statistics. The 0.2 μs neutron capture time difference leads to 0.1% uncorrelated uncertainty of the Gd capture ratio.

3.3 Non-linearity Model

When crossing the acrylic vessel, the particle loses energy in the acrylic, and the remaining energy is deposited in the scintillator. Then the deposited energy is converted to visible light collected by the PMTs, which are readout by the electronics. The energy scale non-linearity is caused by two major sources: the scintillator response and the readout electronics. This non-linearity effect has a minimal impact on oscillation measurement, but is crucial for the measurement of the reactor antineutrino spectra.

The non-linearity from LS is due to the Quenching effect and Cherenkov radiation. Because of this, a semi-empirical electron response model based on Birk's law is chosen to model the scintillator's contribution on the non-linearity. The Daya Bay electronics do not fully capture late secondary PMT hits, and the charge collection efficiency decreases with visible light. This charge non-linearity can not be easily calibrated out on single channel level. Instead, an effective exponential model as a function of total visible energy is used to describe it.
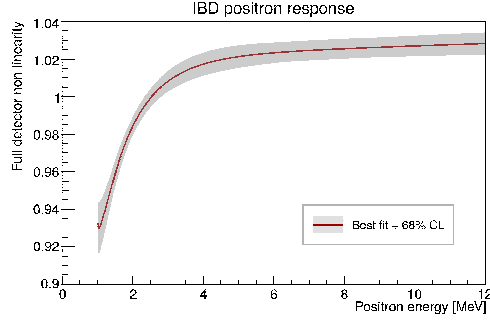
Figure 3: Full IBD positron non-linearity model with 1σ phase space.

Five parameters are used to describe the non-linear response model from LS and PMT read-out electronics including an overall absolute energy scale. An unconstrained 5-parameter fit to γ calibration data and ^{12}B data is done using a χ^2 function. In the χ^2 fit, gammas are connected to the electron scintillator model through MC. This model is also validated with additional calibration data, such as the michel electron spectrum in the high energy region and the continuous $\beta + \gamma$ spectra in the low energy region. In addition, we carried out bench-top measurements of scintillator response using Compton electrons and the readout electronics response using flash ADCs. All these measurements are used to constrain the uncertainty of the non-linearity model.

The full energy response to the positron is computed by adding the visible energy from ionization energy loss and the two annihilation gammas from positrons, assuming that the light produced by ionization is the same as that from electrons. The red line in Fig 3 is the full IBD positron non-linearity model, and the grey band is the 1σ uncertainty band. By utilizing more calibration data to constrain the non-linearity model, the uncertainty of the model is reduced by a factor of two compared to our previous analysis [4].

4. Oscillation Results

4.1 Neutron capture on Gadolinium analysis

The values of oscillation parameters were determined with a χ^2 function constructed with either a covariance matrix or pull terms accounting for the correlation of the systematic errors [6]. The survival probability used in the fit was

$$P_{sur} = 1 - \cos^4\theta_{13}\sin^2 2\theta_{13}\sin^2 2\theta_{12}\sin^2\Delta_{21} - \sin^2 2\theta_{13}(\cos^2\theta_{12}\sin^2\Delta_{31} + \sin^2\theta_{12}\sin^2\Delta_{32}) \quad (4.1)$$

where $\Delta_{ji} \equiv 1.267\Delta m_{ji}^2(eV^2)\frac{L(m)}{E(MeV)}$, and Δm_{ji}^2 is the difference between the mass squares of the mass eigenstates ν_j and ν_i. The last two terms can be combined into a single one with one effective mass splitting Δm_{ee}^2 [4].

Using 217 days of data with six detectors, and 404 days with eight detectors, Fig 4 shows the spectrum deficit in the far site (left) and the allowed regions for the neutrino oscillation parameters at the 68.3, 95.5 and 99.7% confidence levels (right). The best-fit values are $\sin^2 2\theta_{13} = 0.084 \pm$
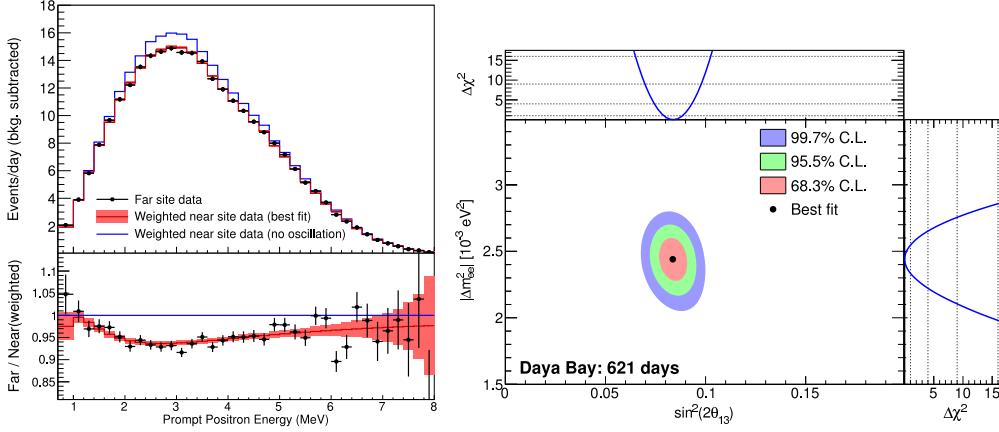
Figure 4: The left figure shows the spectrum deficit in the far site, and the right figure shows the allowed regions for the neutrino oscillation parameters $\sin^2 2\theta_{13}$ and $|\Delta m_{ee}^2|$ at the 68.3, 95.5 and 99.7% confidence levels. The best estimate of the oscillation parameters are given by the black dot.

0.005 and $|\Delta m_{ee}^2| = 2.44^{+0.10}_{-0.11} \times 10^{-3}$ eV^2. Both the covariance-matrix-based fit and nuisance-parameter-based fit yield a consistent result. The precision on θ_{13} is 6%, which makes this angle the best known of all three [1]. The result on $\sin^2 2\theta_{13}$ is consistent with that of other reactor experiments [7, 8]. Under the assumption of normal (inverted) neutrino mass hierarchy, the result of $|\Delta m_{ee}^2|$ is equivalent to $\Delta m_{32}^2 = 2.39^{+0.10}_{-0.11} \times 10^{-3} eV^2$ ($\Delta m_{32}^2 = 2.49^{+0.10}_{-0.11} \times 10^{-3} eV^2$), which is consistent with muon neutrino disappearance experiments [9, 10].

4.2 Neutron capture on Hydrogen analysis

Daya Bay also carried out an independent θ_{13} oscillation analysis using neutron capture on hydrogen. This analysis has high statistics thanks to the additional 22 tons of LS target. This constitutes an independent measurement of the oscillation parameters, as the systematic uncertainties are largely uncorrelated with the analysis using neutron capture on Gadolinium (nGd).

Due to the longer capture time and lower delayed energy, the accidental background is much higher than in the nGd analysis. Two additional cuts are used to deal with this: raising the prompt energy cut (>1.5 MeV), and requiring a prompt to delayed distance cut (<0.5 m). After all cuts, the expected accidental spectrum is subtracted from the total IBD candidate spectrum.

This analysis uses the 217 days of data with six-ADs. A rate-only analysis obtained $\sin^2 \theta_{13} = 0.083 \pm 0.018$, a value consistent with the one from the nGd analysis [11]. As in the nGd analysis, the spectral distortion is consistent with the oscillation hypothesis.

5. Summary

The Daya Bay experiment utilized a relative measurement of $\overline{\nu}_e$ rate deficit and spectrum distortion between near and far detectors to precisely measure $\sin^2 2\theta_{13}$ and $|\Delta m_{ee}^2|$. The remaining two ADs were installed in the summer 2012, and data-taking with all eight detectors begun on Oct 19, 2012. Improved reconstruction and analysis of more calibration data reduced the uncertainty

of the relative energy scale and the energy nonlinearity by a factor of two. The performance of the two new ADs were studied and found to be consistent with others. The correlated background and its uncertainty was significantly reduced thanks to the removal of AmC sources and to an improved estimation method for fast neutrons. With 621 days of data, the best estimates of the oscillation parameters were $\sin^2 2\theta_{13} = 0.084 \pm 0.005$ and $|\Delta m_{ee}^2| = 2.44^{+0.10}_{-0.11} \times 10^{-3}$ eV^2. The precision of $\sin^2 2\theta_{13}$ and $|\Delta m_{ee}^2|$ are expected to be further improved by the end of 2017 to about 3%. Many other analysis are carried out at Daya Bay, and an analysis utilizing neutron capture on hydrogen with the first 217 days of six-AD data measured a consistent result of $\sin^2 2\theta_{13} = 0.083 \pm 0.018$.

6. Acknowledgements

References

[1] http://pdg.lbl.gov/2014/tables/rpp2014-sum-leptons.pdf

[2] M. Apollonio, et al. (CHOOZ Collaboration), Phys. Lett. B, 1999, 466(2-4):415.

[3] F.P.An et al. (Daya Bay Collaboration). Phys. Rev. Lett, 2012, **108**:171803.

[4] F.P.An et al. (Daya Bay Collaboration). Phys. Rev. Lett, 2014, **112**:061801

[5] DayaBay Collaboration, arxiv: hep-ex/0701029, 2007

[6] D. Stump et al. Phys. Rev. D 65, 014012 (Appendix B) (2001).

[7] Y. Abe et al. (Double Chooz Collaboration). Physics Letters B, Volume 735, 30 July 2014.

[8] RENO Collaboration (Seon-Hee Seo for the collaboration). PoS Neutel2013 (2014) 018.

[9] P. Adamson et al. (MINOS Collaboration), Phys. Rev. Lett. 110, 251801 (2013).

[10] K. Abe et al. (T2K Collaboration), Phys. Rev. D 88, 032002 462 (2013).

[11] F.P.An et al. (Daya Bay Collaboration). Phys.Rev. D90 (2014) 071101.